

## Measurement of Coherence-Length Anisotropy in the Isotropic Phase of Nematics

Eric Courtens and Gad Koren\*

*IBM Zurich Research Laboratory, 8803 Rüschlikon, Switzerland*

(Received 6 October 1975)

A phase-sensitive, differential, light-scattering method is used to measure the shape of correlated regions in the isotropic phase of nematics. In MBBA (*p*-methoxybenzylidene *p*-*n*-butylaniline) these regions are elongated along the molecular-axis direction and the critical behavior is close to that predicted by mean-field theory; de Gennes's parameter  $L_2/A$  is positive. In the isotropic phase of the smectic OBBA (*p*-octoxybenzylidene *p*-*n*-butylaniline) the correlated regions are flat and cannot be described by a constant  $L_2$ .

Fluctuations of short-range orientational order in the isotropic phase of liquid crystals give rise to a strong depolarized Rayleigh component in light scattering.<sup>1</sup> Previous measurements of pretransitional behavior on MBBA (*p*-methoxybenzylidene *p*-*n*-butylaniline) indicate an overall increase in scattering intensity,<sup>1</sup> an angular dependence from which a correlation length  $\xi_1$  was obtained,<sup>2,3</sup> and a critical slowing down.<sup>1,4</sup> In principle, the angular and polarization dependence of the scattering intensity can also reveal a possible anisotropy in  $\xi$ , i.e., the shape of the correlated regions.<sup>5</sup> Measurement methods used up to now have not been sufficiently sensitive to extract this information and only an upper bound to the shape parameter  $L_2/A$  of de Gennes<sup>6</sup> is known for MBBA.<sup>2</sup> The first determination of the shape of correlated regions in the isotropic phase is reported here. It was performed on MBBA using a new precise differential light-scattering method based on the difference between  $I_{VH}$  and  $I_{HH}$  for  $90^\circ$  scattering.<sup>7</sup> [ $V$  ( $H$ ) denotes perpendicular (parallel) polarization relative to the scattering plane.] This allowed an independent determination of the critical exponent  $\nu$ . Preliminary results are also reported for OBBA (*p*-octoxybenzylidene *p*-*n*-butylaniline) which has an isotropic-smectic-*A* transition.<sup>8</sup>

The ratio

$$R \equiv \frac{1}{2}(I_{VH} - I_{HH}) / \frac{1}{3}(I_{VH} + 2I_{HH}), \quad \theta = 90^\circ, \quad (1)$$

gives shape information. This is simply seen by substituting in Eq. (1) the Landau-de Gennes expression for the scattered intensity.<sup>5</sup> To order  $q^2$  one obtains  $R = L_2 q^2 / 8A$ , where  $q = (4\pi n \sin \frac{1}{2}\theta) / \lambda$  and  $\theta = 90^\circ$ . This property, however, is independent of the Landau model. It will be shown below on the basis of symmetry alone that  $R$  is proportional to the difference of the square of the two correlation lengths that characterize the problem. A positive value of  $R$  corresponds to

correlations elongated in the direction of high molecular polarizability, i.e., in the direction of the long molecular axis.

The measurement of  $R$  was performed by modulation of the incident polarization and phase-sensitive detection of the scattered light. The method offers the double advantage of being self-calibrating and of allowing easy multiple-scattering corrections. A stable 5-mW He-Ne laser beam (Fig. 1) is sent through a polarizer and a carefully adjusted  $\lambda/4$  plate to obtain circular polarization. A second antireflection-coated  $\lambda/4$  plate is rotated uniformly at frequency  $\Omega$  to produce linear polarization at  $2\Omega$ . This beam is focused on the sample and the transmitted intensity is monitored for detrimental in-phase fluctuations at  $2\Omega$  by a distant photodiode. Dust on the rotating plate produces all harmonics of  $\Omega$  and to eliminate this effect the system is enclosed and slightly overpressured with filtered air. With this precaution, fluctuations in the transmitted intensity are smaller than  $5 \times 10^{-5}$  times the fully modulated signal obtained with a polarizer in front of the photodiode. Moreover, the fluctuations vary slowly in sign, so that the average intensity stability is even greater over the duration of a measurement. The essentials of the detection arm consist of a translatable pinhole ( $S_1$ ) that determines  $\theta$  and the acceptance angle, an analyzer ( $A$ ) that can be accurately and reproducibly placed in the  $V$  or  $H$  position, and an aperture ( $S_2$ ) which determines the length of the scattering region. The discriminated photocounts are accumulated in a multichannel analyzer (MCA) operating in the multiscaler mode and triggered at  $\Omega$ . After a large number of sweeps, the data are transferred to a computer terminal and analyzed in the following way: (i) The strongly modulated signal obtained with the analyzer in position  $V$  is fitted by a constant plus a sine wave at  $2\Omega$ . This yields the depolarization ratio  $R_d \equiv I_{HV} / I_{VV}$  and the phase

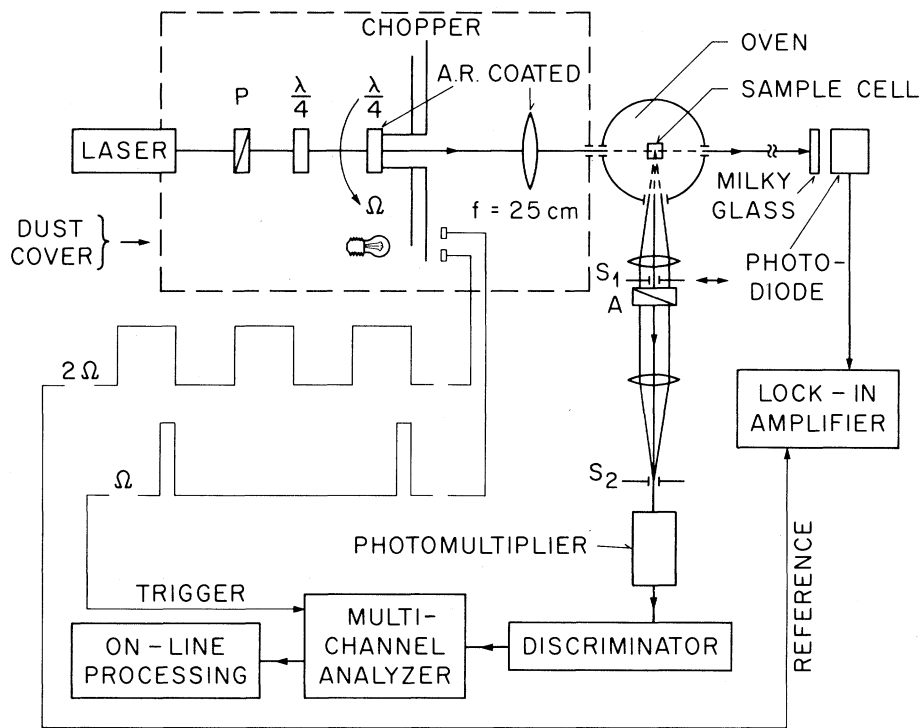


FIG. 1. The experimental system.

and frequency of the reference signal. (ii) The signal obtained with the analyzer in position  $H$  is fitted using the reference information and  $R$  is extracted [Eq. (1)]. Thus, the MCA is used as a sophisticated phase-sensitive detector. The measurement error is obtained from the experimental statistical spread in the photocounts. It is important that the MCA be triggered at  $\Omega$  rather than  $2\Omega$  to prevent  $\Omega$  contributions in the scattered light appearing at  $2\Omega$ . Accurate positions of  $S_1$  and of the analyzer in  $H$  were determined by repeated measurements at a given temperature and changing these variables. The sample was placed in a thermally stabilized oven ( $\pm 0.02^\circ\text{C}$ ). The MBBA<sup>9</sup> was filtered twice through  $0.22\text{-}\mu\text{m}$  Millipore filters into a  $1 \times 1\text{-cm}^2$  cell. The clearing temperature  $T_p$  measured under equilibrium conditions at the beam position in the sample was  $40.22^\circ\text{C}$ . In effect this point is already in the two-phase region and the actual clearing occurs about  $0.1^\circ\text{C}$  above  $T_p$ . The low value of  $T_p$  is due to aging. The OBBA was obtained from Hoffmann-La Roche and not treated further; after a few days it gave  $T_p = 80.1^\circ\text{C}$ .

The ratios  $R$  and  $R_d$  measured in MBBA are shown in Fig. 2. The error bars correspond to 95% confidence limits.  $R$  in MBBA is positive,

meaning that the correlated regions are elongated. In OBBA  $R$  is negative, meaning that the cor-

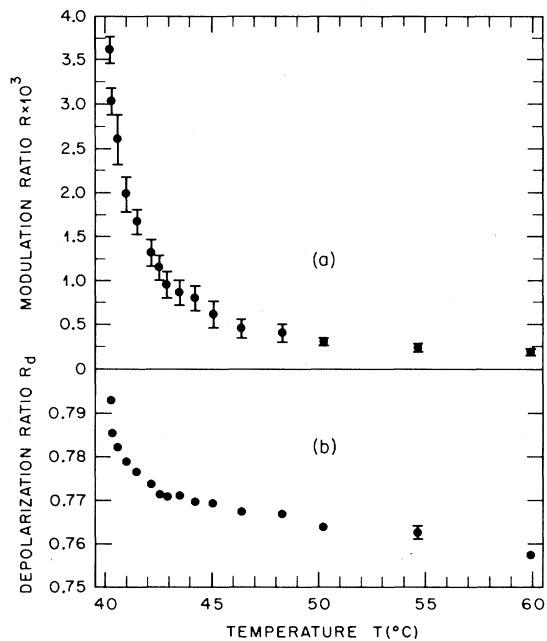


FIG. 2. (a) The modulation ratio  $R$  in MBBA; (b) the depolarization ratio  $R_d$ .

related regions are flat. The raw data from Fig. 2(a) were corrected for multiple scattering using the departure of  $R_d$  from its expected value of  $\frac{3}{4}$ . It is easy to verify that for depolarized scattering a second scattering event scrambles the polarization almost entirely (to better than 97%). Therefore, multiple scattering adds a practically equal contribution  $\delta$  to all polarization components while it attenuates them by an equal factor  $\gamma$ . Hence, if  $J$  is the expected intensity in the absence of multiple scattering and if  $I$  is the measured intensity, one writes  $I_{VV} = \gamma(J_{VV} + \delta)$  and similarly for  $VH$  and  $HH$ . In the absence of scattering due to particulate impurities,  $J_{HV}/J_{VV} = 0.75$ . Such impurities reduce this ratio, in particular at high temperatures. Since the observed ratio is higher than  $\frac{3}{4}$  even far above  $T_p$ , it is reasonable to assume negligible contribution from particulate impurities, and this is confirmed by visual observation.

The corrected values of  $R$  have been fitted with de Gennes's theory  $R = (L_2 q^2 / 8a)(T - T_c)^{-1}$ , where  $A \equiv a(T - T_c)$ , as shown by the straight line (line *a*) in Fig. 3. One finds  $L_2/a = (0.653 \pm 0.036) \times 10^{-12} \text{ cm}^2/\text{C}$  with  $T_p - T_c = 0.98 \pm 0.07^\circ\text{C}$ . The range of error is the 95% confidence limit calculated for this two-parameter fit, taking into account the error bars on the data points. The measured point closest to  $T_p$  (at  $T_p + 0.05^\circ\text{C}$ ) was omitted from all fits as it deteriorated them strongly. At that temperature, the material had already separated into two phases. Using the most recent de-

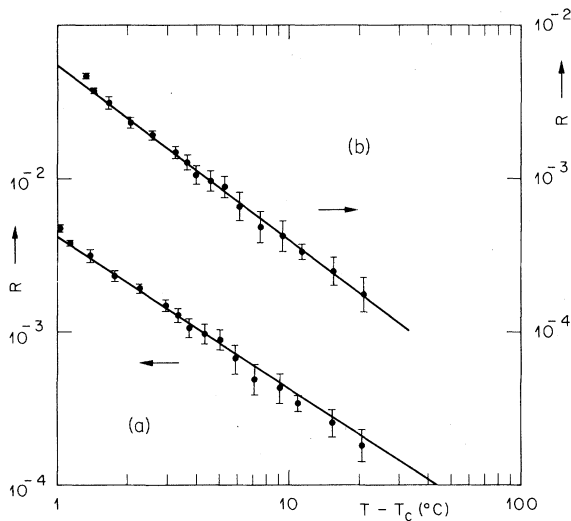


FIG. 3. Line *a*, two-parameter fit to the corrected modulation ratio in MBBA ( $\nu = 0.5$ ); line *b*, three-parameter fit ( $\nu = 0.57 \pm 0.09$ ).

termination of  $L_1/a$  in MBBA,<sup>3</sup>  $(0.97 \pm 0.08) \times 10^{-12} \text{ cm}^2/\text{C}$ , and the present value of  $L_2/a$ , one calculates the two correlation lengths that characterize the problem,  $\xi_n^2 = (L_1 + \frac{2}{3}L_2)/A$  and  $\xi_t^2 = (L_1 + \frac{1}{8}L_2)/A$ .<sup>6</sup> One finds  $\xi_n = 119(T - T_c)^{-1/2} \text{ \AA}$  and  $\xi_t = 104(T - T_c)^{-1/2} \text{ \AA}$ . The coherence-length anisotropy in MBBA is thus rather small ( $\sim 15\%$ ) which explains why it could not be detected in previous measurements. In particular, our value of  $L_2/a$  is well below the upper bound given by Stinson and Litster.<sup>2</sup>

A close examination of line *a* of Fig. 3 suggests that a slightly different slope might give a better fit for MBBA. On the other hand, in OBBA, where critical scattering is also observed, the results cannot possibly be fitted with a constant  $L_2$ . It is thus relevant to obtain an expression for  $R$  independent of the Landau theory. The depolarized Rayleigh wing intensity is  $I \propto \sum_{ijkl} \bar{G}_{ijkl} \times m_i n_j \bar{m}_k n_l$ , where  $\bar{G}$  is a correlation tensor and  $\bar{m}$  and  $\bar{n}$  are the polarization vectors of the incident and scattered fields, respectively.<sup>10</sup> Here

$$G_{ijkl}(\vec{q}) = (2\mathcal{N})^{-1} \langle \sum_{a,b} \bar{\alpha}_{ij}^a \alpha_{kl}^b \exp[-i\vec{q} \cdot (\vec{r}_a - \vec{r}_b)] \rangle,$$

where  $\bar{\alpha}^a$  is the traceless part of the molecular polarizability of molecule *a* at position  $\vec{r}_a$ ,  $\vec{q}$  is the momentum exchanged in scattering, and the sum extends over all pairs in a volume containing  $\mathcal{N}$  molecules. In a liquid,  $\bar{G}(\vec{q})$  has cylindrical symmetry about  $\vec{q}$ . Taking for convenience  $\vec{q}$  parallel to the third axis,  $\bar{G}$  has six distinct components, i.e.,  $G_{11}$ ,  $G_{33}$ ,  $G_{44}$ ,  $G_{66}$ ,  $G_{12}$ , and  $G_{13}$  (in abbreviated subscript notation). From cylindrical symmetry  $G_{66} = \frac{1}{2}(G_{11} - G_{12})$ , whereas from tracelessness in the first pair of indices  $G_{13} = -\frac{1}{2}G_{33}$  and  $G_{12} = \frac{1}{2}G_{33} - G_{11}$ . This leaves three independent components. However, if  $\bar{G}$  is expanded up to second order in  $\vec{q}$ , the isotropy of the tensor  $\langle \sum_{a,b} \bar{\alpha}^a \alpha^b (\vec{r}_a - \vec{r}_b)(\vec{r}_a - \vec{r}_b) \rangle$  leads to the additional relation  $G_{44} = \frac{1}{4}G_{11} + \frac{1}{2}G_{33}$ . Hence, correlations small with respect to  $q^{-1}$  are described in all generality by two independent parameters (which in de Gennes's model are related to  $L_1/A$  and  $L_2/A$ ). Keeping  $\vec{q}$  in the third direction, and with a judicious choice of axis, one obtains for  $90^\circ$  scattering  $I_{VV} \propto \frac{5}{8}G_{11} + \frac{1}{8}G_{33}$ , and  $I_{HH} \propto \frac{1}{4}G_{11} + \frac{1}{2}G_{33}$ , or  $R = \frac{1}{2}(G_{11} - G_{33})/(G_{11} + G_{33})$ . To order  $q^2$  the correlation function  $G_{ii}(\vec{q})$  allowed by symmetry is proportional to  $[1 + \xi_i^2(q_j^2 + q_k^2) + \xi_n^2 q_i^2]^{-1}$ , where  $(i, j, k)$  is any permutation of  $(1, 2, 3)$ .

Hence, to order  $q^2$ ,

$$R = \frac{1}{4}(\xi_n^2 - \xi_t^2)q^2. \quad (2)$$

It is thus apparent that  $R$  determines the differ-

ence of the squares of the correlation lengths in two directions. With the appropriate  $\xi_n$  and  $\xi_t$ , the Landau result is, of course, recovered.

A three-parameter fit of the corrected values of  $R$  for MBBA by the function  $C(T - T_c)^{-2\nu}$  gives  $\nu = 0.57 \pm 0.09$  and  $T_p - T_c = 1.27 \pm 0.36^\circ\text{C}$ . Again the range of errors is the 95% confidence limit. This fit is shown in Fig. 3 as line *b*. The multiple-scattering correction does not affect the best value of  $\nu$  and only increases  $T_c$ . Examination of Fig. 3 suggests that the departure of  $\nu$  from 0.5 might be significant. However in view of the error bar it is difficult to ascertain a real departure from mean-field theory.<sup>11</sup> The peculiar behavior in OBBA suggests further study of the coupling between nematic and smectic ordering in the isotropic phase. The coupling leads to a departure from the simple phenomenological theory already observed for the scattered intensity and the linewidth,<sup>12</sup> but our results indicate that  $\xi_n^2 - \xi_t^2$  is for OBBA a much more sensitive quantity than the scattered intensity itself.

In conclusion, the first measurement of  $L_2/a$  in the isotropic phase of a liquid crystal has been obtained. The sensitive method described here is expected to find applications in the study of liquid crystals, homologous series, and other depolarized scattering studies.

The participation of Aasmund Sudbø in the early stages of the present work is gratefully acknowledged. Many thanks also go to Dr. M. Schadt for kindly supplying the OBBA sample, to Mr. H. Amrein for his technical assistance, and to Profes-

or J. Feder and Professor K. A. Müller for a critical reading of the manuscript.

\*Present address: Physics Department, Technion, Haifa, Israel.

<sup>1</sup>T. W. Stinson and J. D. Litster, Phys. Rev. Lett. **25**, 503 (1970).

<sup>2</sup>T. W. Stinson and J. D. Litster, Phys. Rev. Lett. **30**, 688 (1973).

<sup>3</sup>E. Gulari and B. Chu, J. Chem. Phys. **62**, 798 (1975).

<sup>4</sup>G. K. Wong and Y. R. Shen, Phys. Rev. A **10**, 1277 (1974).

<sup>5</sup>T. W. Stinson, J. D. Litster, and N. A. Clark, J. Phys. (Paris), Colloq. **33**, C1-69 (1972).

<sup>6</sup>P. G. de Gennes, Mol. Cryst. Liq. Cryst. **12**, 193 (1971).

<sup>7</sup>Its origin should be distinguished from the "Krishnan effect" [R. S. Krishnan, Proc. Indian Acad. **A1**, 211 (1934)], produced by Mie scattering from large molecules or aggregates, which is negligible here.

<sup>8</sup>J. B. Flannery, Jr., and W. Haas, J. Phys. Chem. **74**, 3611 (1970).

<sup>9</sup>Eastman Chemicals X11246, specially purified grade.

<sup>10</sup>L. D. Landau and E. M. Lifshitz, *Electrodynamics of Continuous Media* (Pergamon, Oxford, England, 1960), Chap. 14.

<sup>11</sup>A brief account of a theoretical study of critical behavior in the isotropic phase of nematics has been given by T. Lubensky and R. G. Priest, Phys. Lett. **48B**, 103 (1974).

<sup>12</sup>T. R. Steger, Jr., J. D. Litster, and W. R. Young, in *Liquid Crystals and Ordered Fluids*, edited by J. F. Johnson and R. S. Porter (Plenum, New York, 1974), Vol. 2, p. 33.

## Vortex Velocity in Turbulent He II Counterflow\*

R. A. Ashton and J. A. Northby

*Department of Physics, University of Rhode Island, Kingston, Rhode Island 02881*

(Received 8 October 1975)

We have used the ion-vortex interaction to measure the drift velocity of the vorticity present in turbulent counterflow, and find that it moves in the direction of normal-fluid flow. The result is in direct conflict with a central assumption of the presently accepted model of the turbulent state.

Recent work on turbulence in He II counterflow has shown that the model first proposed by Vinen<sup>1</sup> to account for second-sound attenuation is also able to give a reasonable description of critical velocities,<sup>2</sup> ion trapping,<sup>3</sup> and noise on second-sound signals.<sup>4</sup> The principal assumptions of this model are (1) the superfluid state consists

of an homogeneous, isotropic, tangled mass of vortex lines. (2) The vorticity is geometrically similar at all times and therefore may be characterized by  $L_0$ , the length of line per unit volume. (3) The state is maintained by a dynamic balance between growth and annihilation processes; dimensional arguments then serve to pre-